Correlating the properties of amorphous silicon with its flexibility volume

Zhao Fan,[1] Jun Ding,[2,*] Qing-Jie Li,[1] and Evan Ma[1,*]

[1]*Department of Materials Science and Engineering, Johns Hopkins University, Baltimore, Maryland 21218, USA*

[2]*Materials Sciences Division, Lawrence Berkeley National Laboratory, Berkeley, California 94720, USA*

(Received 13 February 2017; revised manuscript received 24 March 2017; published 28 April 2017)

For metallic glasses, "flexibility volume" has recently been introduced as a property-revealing indicator of the structural state the glass is in. This parameter incorporates the atomic volume and the vibrational mean-square displacement, to combine both static structure and dynamics information. Flexibility volume was shown to quantitatively correlate with the properties of metallic glasses [J. Ding *et al.*, Nat. Commun. **7**, 13733 (2016)]. However, it remains to be examined if this parameter is useful for other types of glasses with bonding characteristics, atomic packing structures, as well as properties that are distinctly different from metallic glasses. In this paper, we tackle this issue through systematic molecular-dynamics simulations of amorphous silicon (a-Si) models produced with different cooling rates, as a-Si is a prototypical covalently bonded network glass whose structure and properties cannot be characterized using structural parameters such as free volume used for metallic and polymeric glasses. Specifically, we demonstrate a quantitative prediction of the shear modulus of a-Si from the flexibility for atomic motion. This flexibility volume descriptor, when evaluated on the atomic scale, is shown to also correlate well with local packing, as well as with the propensity for thermal relaxations and shear transformations, providing a metric to map out and explain the structural and mechanical heterogeneity in the amorphous material. This case study of a model of covalently bonded network a-Si, together with our earlier demonstration for metallic glasses, points to the universality of flexibility volume as an indicator of the structure state to link with properties, applicable across amorphous materials with different chemical bonding and atomic packing structures.

DOI: 10.1103/PhysRevB.95.144211

I. INTRODUCTION

For amorphous solids, quantitative property correlations have been difficult to come by, lagging far behind conventional crystalline materials. An example is the widely used amorphous silicon (a-Si). a-Si can be prepared via a number of processing routes, the most popular being chemical or physical vapor deposition [1–3]. Other routes include ion irradiation [4,5] or mechanical deformation [6] of crystalline silicon. The resultant amorphous structures are all different, and so are their shear rigidity and deformability (e.g., some a-Si are brittle while others can be plastically deformed [6–8]). It remains a challenge to define a parameter that can be used to quantitatively link properties.

For metallic or polymeric glasses, free volume is widely cited as a structural parameter to correlate with properties [9,10]. For example, a rapidly quenched metallic glass is believed to contain more free volume than a slowly cast one and is thus less rigid and more prone to flow. However, this picture is obviously invalid for a-Si, which is a prototypical covalently bonded network amorphous material. Here faster cooling from liquid actually retains a higher-density glass, containing less open volume (see Refs. [7,8]); but the resultant structure is more metallic- and liquidlike, making the glass more amenable to shear flow. Conversely, slower cooling leads to a network glass with a relatively open structure, but the material is stronger. More discussion on the inadequacy of excess atomic volume to reflect the deformability of a-Si will be presented later in this paper.

Fictive temperature [11,12] is another commonly used concept in the field of glass research, for representing the level of disorder in a glassy material. But this parameter is not descriptive of the atomistic origin of a property, and needs to be mapped to some other real physical quantities such as potential energy for it to be computed or measured. In terms of correlating with properties, a glass with a lower fictive temperature has a lower potential energy, and is usually stronger and has a higher elastic modulus. However, there are also cases where a glass has a higher energy and higher fictive temperature [13,14] but is more kinetically stable because the glass is in a potential energy valley with a higher curvature, leading to a higher glass transition temperature [15] and also a higher elastic modulus and strength. In other words, fictive temperature is only correlated with thermodynamic stability but not necessarily with kinetic stability and strength/modulus. In the case of a-Si, faster quenching from liquid [7,8] results in an amorphous structure that is higher in energy, more metallic- and liquidlike, and hence more deformable and less stiff. This could perhaps be depicted as corresponding to a higher fictive temperature; nonetheless there is no equation that can directly predict modulus or strength, based on the fictive temperature or potential energy of the a-Si in question.

Simulating the a-Si model employing the Stillinger-Weber (SW) potential [16], Demkowicz and Argon showed that depending on the cooling rate used to quench from liquid silicon, the resultant a-Si models exhibit different elastic moduli, yield-point behavior, and flow stresses [7,8]. These differences can be attributed to different fractions of liquidlike atomic environments, ϕ, in the amorphous structure [7,8]. The liquidlike atoms were defined based on their nearest-neighbor bond-angle distribution that resembles liquid Si. However, while this structural descriptor is useful in explaining the

*Corresponding authors: ding@lbl.gov; ema@jhu.edu

property trend from the structural state the a-Si is in, again the challenge remains as to how to quantitatively derive from the descriptor a property such as shear modulus or strength.

Very recently, Ding *et al.* [17] introduced a new indicator of the structural state, termed the "flexibility volume," which is assessed via combining both atomic volume and atomic vibrations that probe local configurational space. This parameter incorporating local structure and local dynamics was developed for metallic glasses (MGs), a class of amorphous materials characterized by metallic bonding. A systematic study on a variety of MGs has demonstrated that the flexibility volume can deterministically predict the shear modulus, and strongly correlate with various properties on both atomic and macroscopic levels. However, it is unclear if the same holds for a-Si, the amorphous material focused on in this paper. Specifically, the a-Si structure is a covalently bonded continuous random network (CRN), and loosely packed with a coordination number (CN) of ~4–6 [16,18–20]. This is very different from the densely packed MGs with nondirectional bonds that result in a high CN often of the order of 12 [21]. Moreover, free volume is often cited to characterize MGs, but not applicable to a-Si as discussed earlier. Therefore, it would be interesting and important to examine the validity of applying the flexibility volume parameter to a-Si; this would not only provide a useful indicator for establishing correlations with properties in a-Si, but also validate the concept of flexibility volume as a universal parameter for different classes of amorphous materials characterized by a variety of electronic bonding and atomic packing structures.

II. METHODS

Molecular-dynamics (MD) simulations [22] have been employed to prepare and analyze the a-Si samples using the SW potential [16], which has been extensively utilized to model the structure and properties of a-Si (this potential is believed to be adequate to construct a representative model of a-Si for our purposes; we are aware that additional tweaking of the prefactor for the three-body term in the potential can change the degree of bond directionality, which was found to affect the coordination number of local defects and/or their behavior in plastic arrangements in similar network amorphous solids [23]). Our a-Si model contains 85184 atoms, i.e., $22\times22\times22$ cubic unit cells of the diamond cubic configuration, under periodic boundary conditions (PBCs). The samples were quenched to room temperature (300 K) from equilibrium liquids above the melting point. The quenching was performed using a Nose-Hoover thermostat with zero external pressure, over a range of cooling rates from 5.0×10^{10} to 5.0×10^{13} K/s. The average atomic volume (Ω_a) of those simulated a-Si, increasing with decreasing cooling rate (note that this is opposite to the trend for MGs), is shown in Fig. 1.

Each sample was kept at equilibrium under a microcanonical ensemble (*NVE*) at room temperature to calculate the atomic vibrational mean-square displacement (MSD). The MSD of the ith atom is defined as $\langle[x_i(t)-\bar{x}_i]^2\rangle$, where $\bar{x}_i$ is the equilibrium (time-averaged) position of the ith atom, and the MSD is evaluated on short time scales when the MSD is flat with time and thus contains the vibrational but not the diffusional contribution [17] [see Fig. 2(a)]. The calculated

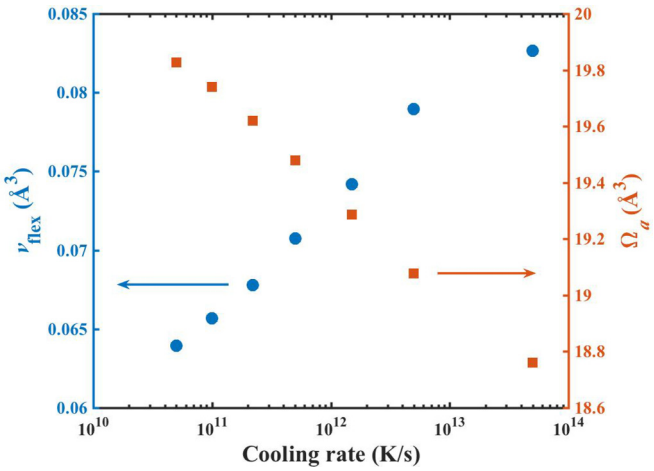

FIG. 1. The system-averaged flexibility volume $v_{\rm flex}$ and atomic volume Ω_a as a function of cooling rate for a-Si samples prepared using various cooling rates (q, in K/s) from liquid.

MSD was taken by averaging over 100 independent runs, all starting from the same configuration but with momenta assigned randomly from the appropriate Maxwell-Boltzmann distribution [17,24]. Voronoi tessellation [25] was employed to obtain the atomic volume (Ω_a).

The vibrational anisotropy (η_i) of the ith atom is calculated by monitoring the time-dependent $n_i(t)=x_i(t)-\bar{x}_i$, where $n_i(t)$ is the Euclidean vector to describe the corresponding atomic vibration. The average of fabric tensor $F=\langle n_i(t)\otimes n_i(t)\rangle$ for the ith atom yields three eigenvalues, λ_k ($k=1,2,3$). Then the vibrational anisotropy can be defined as $\frac{3}{\sqrt{6}}\sqrt{\sum_{k=1}^{3}(\lambda_k-\frac{1}{3})^2}$. For the isotropic case, $\lambda_1=\lambda_2=\lambda_3=\frac{1}{3}$, so $\eta_i=0$. For the extremely anisotropic case, e.g., one-dimensional atomic vibration, $\lambda_1=1$ and $\lambda_2=\lambda_3=0$, then $\eta_i=1$.

Simple shear deformation at a strain rate of $10^8\,{\rm s}^{-1}$ was applied on a-Si samples prepared at various cooling rates. During the shear deformation, the box was deformed by supercell tilting followed by MD relaxation, with a step length of 1×10^{-7} in shear strain. The shear stress-strain curves are shown in Fig. 2(b). The shear modulus G of a-Si models was derived from the shear stress-strain curves at small (0.5%) strain (around which the G value levels off to a steady value) and averaged over simple shear deformation along different directions (i.e., $\pm xy,\pm xz,\pm yz$). Our studied a-Si samples are large enough (containing 85184 atoms) to achieve the converged G in the calculation.

The activation-relaxation technique (ART nouveau) in MD simulations [17,26–28] was used to investigate the energy barrier for thermally activated relaxation events in the a-Si sample quenched to room temperature from liquid at 1×10^{11}K/s. To initiate the local excitations of the system, small perturbations in ART were introduced by applying random displacement on a small group of atoms (an atom and its nearest neighbors with a distance cutoff of 3.0 Å). The magnitude of displacement was fixed, while the direction was randomly chosen. The system was pushed toward the saddle point using the Lanczos algorithm, when the curvature

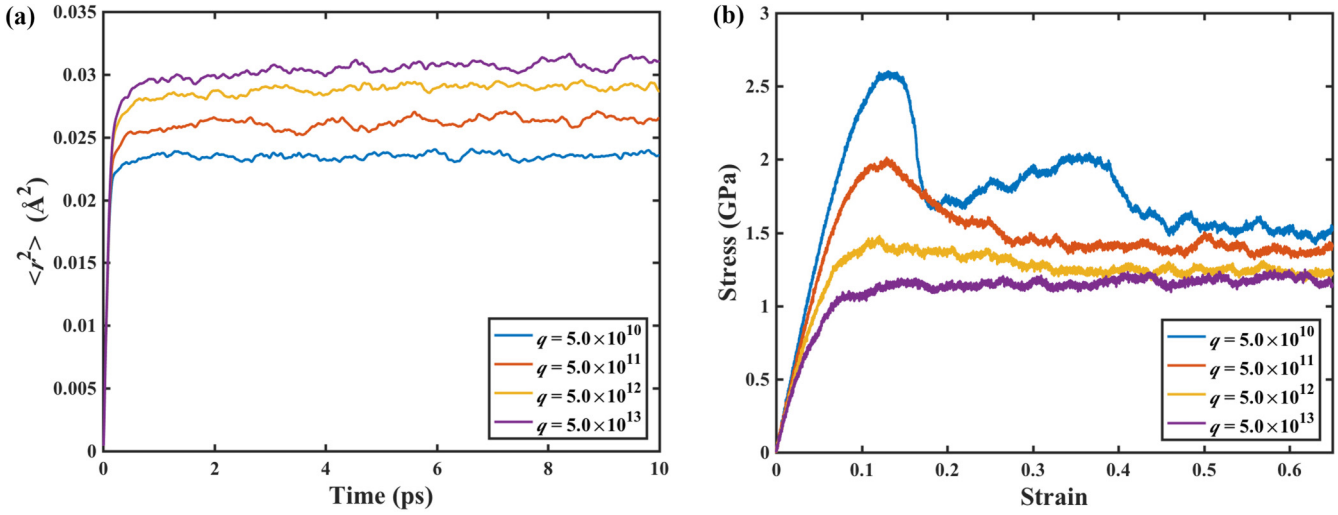

FIG. 2. For a-Si configurations prepared using various cooling rates (q, in K/s) from liquid. (a) MSD, $\langle r^2 \rangle$, as a function of time. $\langle r^2 \rangle$ is evaluated on these short time scales and thus contains the vibrational but not the diffusional contribution. (b) MD-simulated stress-strain curves under simple shear loading with strain rate of 10^8 s^{-1}.

of potential energy landscape was found to overcome the chosen threshold. A total of ∼150000 different activations were identified for that a-Si sample, after removing the failed searches and redundant saddle points.

III. RESULTS AND DISCUSSION

A. The flexibility volume

As introduced before [17], the flexibility volume is defined as $\upsilon_{\text{flex}} = \langle r^2 \rangle a$, where a is the average atomic spacing, given by $a = \sqrt[3]{\Omega_a}$, Ω_a is the average atomic volume, and $\langle r^2 \rangle$ is the atomic vibrational mean-square displacement [in the regime where it is flat with time, as shown in Fig. 2(a)]. This structure parameter is unlike all other previous ones, as it combines the structural information of both the atomic volume and the space accessed by atomic vibration, the two together quantitatively determining the shear modulus G of a-Si (as shown below in Sec. III B). The flexibility volume can in fact be evaluated on each and every atom (the ith atom), $\upsilon_{\text{flex},i}$, and υ_{flex} of the sample (or local region) is then an average of all the $\upsilon_{\text{flex},i}$ in the system (region).

As shown in Fig. 1, the flexibility volume of a-Si undergoes obvious changes with the cooling rate used to prepare the amorphous sample. The trend that υ_{flex} decreases with slower cooling rate is consistent with the case for MGs [17]. But, as mentioned earlier, unlike MGs the a-Si with slower cooling rate (equivalently with lower internal energy) exhibits larger volume (or lower density). The opposite trends between the flexibility volume and atomic volume for a-Si (see Fig. 1) bring forth an interesting scenario: a larger surrounding elbow room ($\Omega_{a,i}$ or the system average Ω_a) can actually be accompanied by a smaller wiggle space accessed via vibration (smaller MSD, $\upsilon_{\text{flex},i}$ and υ_{flex}). To better explain this seemingly anomalous behavior, we also calculated the vibrational anisotropy (η) of the ith atom, by monitoring the time-dependent atomic oscillation (see Sec. II). As shown in Fig. 3(a), for a-Si, the larger the flexibility volume, the greater the vibrational anisotropy. The latter is apparently a major contributor to the flexibility volume. For instance, the packing distortion around an atom entails looser directions and an easier pathway for atomic movement, and consequently higher vibrational anisotropy, leading to larger flexibility volume. Conversely, a well-defined and strongly bonded local motif such as tetrahedrally coordinated Si reduces anisotropy, and decreases flexibility, even though the surrounding space is enlarged. This can be confirmed by calculating the average vibrational anisotropy for CN = 4 and CN > 4, which are 0.151 and 0.218, respectively (in the a-Si sample quenched using a cooling rate of 5.0×10^{11} K/s).

We note that the flexibility volume evaluated for individual atoms, i.e., $\upsilon_{\text{flex},i}$, is not uniformly and randomly distributed across the a-Si sample. Instead, a spatial correlation is revealed in Fig. 3(b), by employing the spatial correlation function, $C_{\text{flex}}(r)$. A similar function of nonaffine displacement was used before to indicate the size of shear transformation zones in MGs [29]. We define $C_{\text{flex}}(r)$ as

$$C_{\text{flex}}(r) = \frac{\sum_{i\leqslant j} \upsilon_{\text{flex},i}\upsilon_{\text{flex},j} n(r - r_{ij})}{\sum_{i\leqslant j} n(r - r_{ij})} - \frac{\left[\sum_{i\leqslant j} \upsilon_{\text{flex},i} n(r - r_{ij})\right]\left[\sum_{i\leqslant j} \upsilon_{\text{flex},j} n(r - r_{ij})\right]}{\left[\sum_{i\leqslant j} n(r - r_{ij})\right]^2}, \quad (1)$$

where r_{ij} is the distance between the ith and jth atoms, and the function $n(x) = \begin{cases} 1, |x| \leqslant \frac{1}{2}\Delta \\ 0, |x| > \frac{1}{2}\Delta \end{cases}$ [Δ is the width of the bins used in calculating and plotting $C_{\text{flex}}(r)$; see Fig. 3(b)]. The spatial correlation functions of flexibility volume, for a-Si prepared with various cooling rates, decreases with increasing distance r. Following Ref. [29], the corresponding correlation length, as indicated in Fig. 3(b), is the distance where spatial correlation vanishes. For all four samples prepared with different cooling rates, this correlation length for a-Si is at ∼1 nm, which is

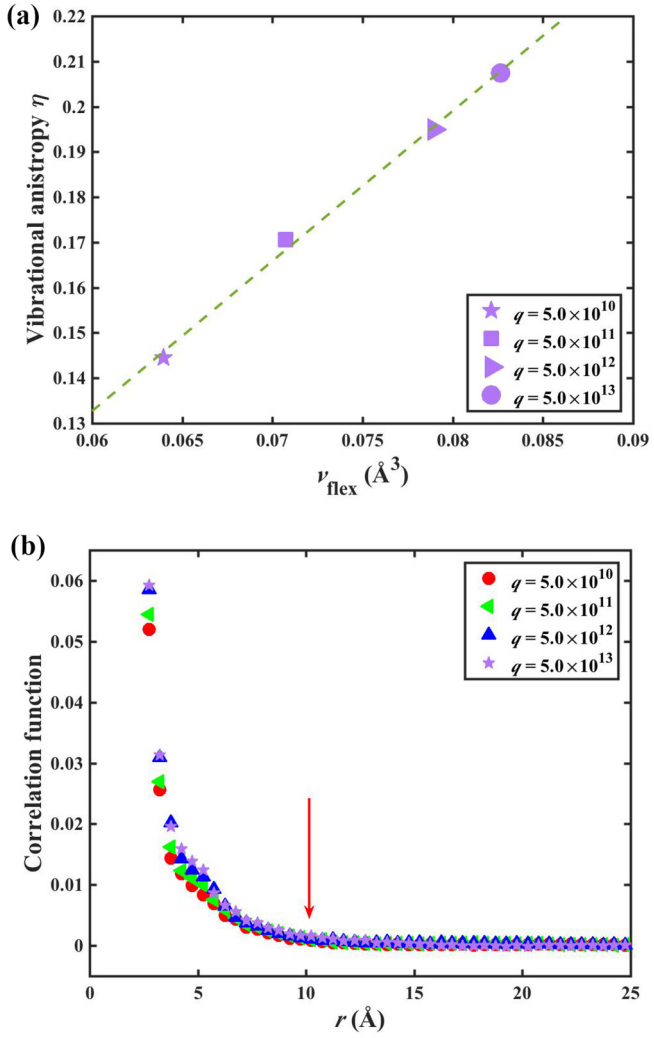

FIG. 3. Four a-Si configurations prepared using different cooling rates (q, in K/s) from liquid. (a) System-averaged vibrational anisotropy η versus flexibility volume. (b) Spatial correlation function of the atomic flexibility volume for a-Si configurations. The correlation length is around 1 nm, as indicated by the red arrow.

consistent with the approximate size of shear transformation zones in a-Si (Refs. [8,30,31]). This implies an underlying link between the local structure (in terms of flexibility volume) and shear transformation in a-Si (more discussions in Sec. III D).

B. The v_{flex}–G correlation

We probe into the correlations based on flexibility volume, by first quantitatively determining the shear modulus G of a-Si. Here G is taken as our primary target because it is widely regarded as a key baseline property that controls the energy barrier for relaxation and shear flow [32,33]. G is also known to depend strongly on glass configuration, and hence on processing history [34]: the slower the cooling rates, the higher the G [as reflected by the steeper slope of stress-strain curve in Fig. 2(b)]. The connection between G and the atomic MSD, $\langle r^2\rangle$, was recognized before [35] but has not been quantitatively verified using systematic data, let alone for different types of glasses. Moreover, we have shown recently that MSD alone is actually not universally deterministic of G, but flexibility volume is [17].

For an isotropic Debye solid, the Debye temperature θ_D can be expressed as [32]

$$\theta_D = \frac{h}{k_B}\left(\frac{4\pi}{9}\right)^{-1/3}(\Omega_a)^{-1/3}\left(\frac{1}{v_l^3}+\frac{2}{v_s^3}\right)^{-1/3}, \quad (2)$$

where $v_l = \sqrt{(B+\frac{4}{3}G)/\rho}$ and $v_s = \sqrt{\frac{G}{\rho}}$ are the longitudinal and transverse sound velocities, respectively, B is the bulk modulus, and $\rho = \frac{m}{\Omega_a}$ is the mass density, where m is average atomic weight. For SW a-Si [16], B/G is in the range of 3.21–4.81. Thus the cases we are dealing with are those for which $B = (4.0 \pm 0.8)G$. Over this range, approximating $B = 4G$ would only involve an error of no more than ~1% in θ_D, because in Eq. (2) the second term in the last bracket overrides by far the first term. Hence Eq. (2) can be simplified to

$$\theta_D \approx \frac{h}{k_B}\left(\frac{4\pi}{9}\right)^{-1/3}(2.082)^{-1/3}(\Omega_a)^{-1/3}\sqrt{\frac{G}{\rho}}. \quad (3)$$

Now, recall that the Debye temperature is also known to scale with the vibrational MSD, $\langle r^2\rangle$, following [36]

$$\theta_D^2 = \frac{9\hbar^2 T}{m k_B \langle r^2\rangle}. \quad (4)$$

Combining Eqs. (2), (3), and (4), we arrive at [17]

$$G = C_{Si}\frac{k_B T}{\langle r^2\rangle a} = C_{Si}\frac{k_B T}{v_{flex}}, \quad (5)$$

where k_B is the Boltzmann constant and the constant $C_{Si} = \frac{9}{4\pi^2}(\frac{4\pi}{9})^{2/3}(2.082)^{2/3} = 0.464$. Note that G in Eq. (5) contains no viscoelastic relaxation. This derivation conveys the idea that high-frequency, atomic-level vibrations contain a signature of

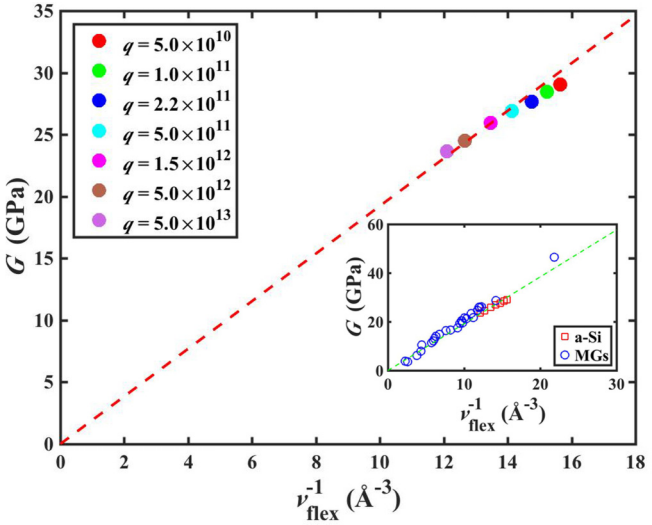

FIG. 4. Quantitative correlation between the shear modulus G and the flexibility volume v_{flex} for a-Si obtained using different quench rates q, in K/s. The inset includes all the data points for a-Si (present work) and MGs (from Ref. [17]). The dashed red straight line (green in the inset) is the prediction derived in Eq. (5).

long-wavelength phonons which depend on G. The equation predicts that at a given temperature T (e.g., room temperature), a single structural parameter υ_{flex} can be used to predict the shear modulus (in the current paper, for a-Si). In other words, once the structural descriptor υ_{flex} is quantified via computational or experimental measurement for a-Si samples that have been processed differently to give rise to different υ_{flex}, a quantitative correlation is available to gauge and compare the mechanical response G of these various a-Si. In the following, we will demonstrate that Eq. (5) indeed holds for a-Si.

Figure 4 plots G versus υ_{flex}.The error bar for the group of data used for averaging is smaller than the size of each data point shown in the plot. The dataset demonstrates a strong correlation, and in fact conforms within ~3% to the linear relationship predicted in Eq. (5), which is the straight dashed line in Fig. 4 (the slope of this line itself has an error margin of ~2%, from the uncertainty in B/G or ν_l/ν_s in the approximation used in the derivation of the above equations). The small error in our dataset (<3%) may also be partly from the method used to derive G, i.e., taking the slope of the shear stress-strain curve at 0.5% strain. Figure 4 establishes that υ_{flex} is all that is needed to account for G quantitatively, allowing prediction and comparison for various a-Si prepared under different conditions. This conclusion is consistent with that reported for MGs [17]. As seen in the inset of Fig. 4, which includes the dataset for MGs as well as that for the a-Si samples studied here, the prediction given in Eq. (5) (dashed line) is an adequate representation of all the data (in other words, C_{Si} here is practically the same as the constant C known for all MGs [17]). This observation of a single flexibility volume parameter to quantitatively correlate with the mechanical response of different amorphous materials is very interesting. In contrast, all other structural metrics used before, even in cases where they themselves are quantifiable (e.g., fraction of liquidlike sites ϕ, or potential energy, or excess volume over a reference such as the corresponding crystal, or even the absolute value of free volume if that is actually quantifiable by some means), cannot be plugged into an equation to directly calculate a particular property.

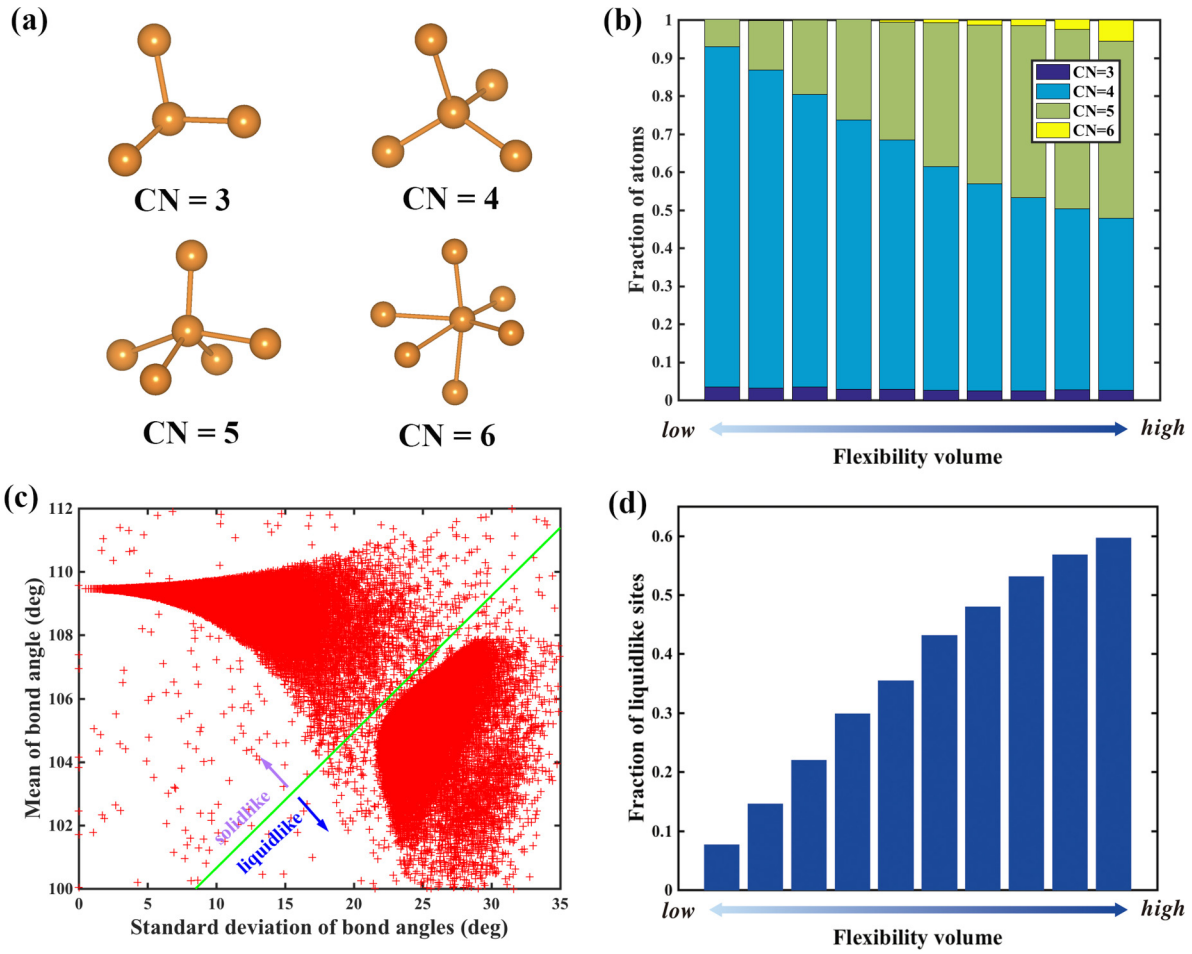

FIG. 5. Correlation between flexibility volume υ_{flex} and static structural indicators for a-Si. For the a-Si with the cooling rate of 5.0×10^{11}K/s, (a) illustration of examples of atomic sites in a-Si with different CN; (b) correlation between the flexibility volume and the fraction of atomic sites with different CN (from CN = 3 to CN = 6). All the atoms are sorted, from left to right, based on flexibility volume $\upsilon_{\text{flex},i}$ into bins each containing 10% all of the atoms; (c) mean bond angles and their corresponding standard deviation for all the atomic sites; the solidlike and liquidlike sites can be separated accordingly; (d) correlation between the flexibility volume and the fraction of liquidlike sites. All the atoms are sorted based on flexibility volume $\upsilon_{\text{flex},i}$ into bins each containing 10% of all the atoms.

C. Correlating v_{flex} with atomic-level static structure

Next we connect the static atomic-level structure of a-Si with the flexibility volume. Two static structural indicators at the atomic level, the CN and fraction of liquidlike sites, are commonly used for a-Si [16,37]. Several examples of atomic sites in a-Si with different CN (CN = 3–6) are plotted in Fig. 5(a). In comparison, crystal Si (c-Si) has the tetrahedral packing with CN = 4, which is also regarded as the favored local motif in a-Si. Several decades ago, the defects in a-Si were originally hypothesized to be undercoordinated sites (e.g., CN = 3), referred to as "dangling bonds" [38,39]. But more recent findings have indicated that overcoordinated sites (e.g., CN = 5) are more defectlike and liquidlike [7,37,40]. As presented in Fig. 5(b), the atomic flexibility volume in a-Si correlates predominantly with CN = 5 (the fractions of CN = 3 and CN = 6 are negligible): more CN = 5 at the expense of CN = 4 corresponds to larger atomic flexibility volume. The other static atomic-level structural indicator for a-Si is the liquidlike sites. These sites were characterized by Demkowicz and Argon according to the mean bond angle as well as its standard deviations (see details in Refs. [7,37]). Following this practice, we analyzed the bond angles in our a-Si in Fig. 5(c), where liquidlike and solidlike atomic sites can be well separated. Interestingly, as shown in Fig. 5(d), the flexibility volume exhibits a strong correlation with the fraction of liquidlike sites ϕ: the larger the flexibility volume, the higher the fraction of liquidlike sites. All these analyses indicate that the flexibility volume reflects very well the existing static structural indicators at the atomic level. But the new parameter of flexibility volume brings unprecedented advantages: it offers not only another way to quantitatively identify the liquidlike sites (more defectlike sites), but also a descriptor of structure state that can deterministically predict the shear modulus.

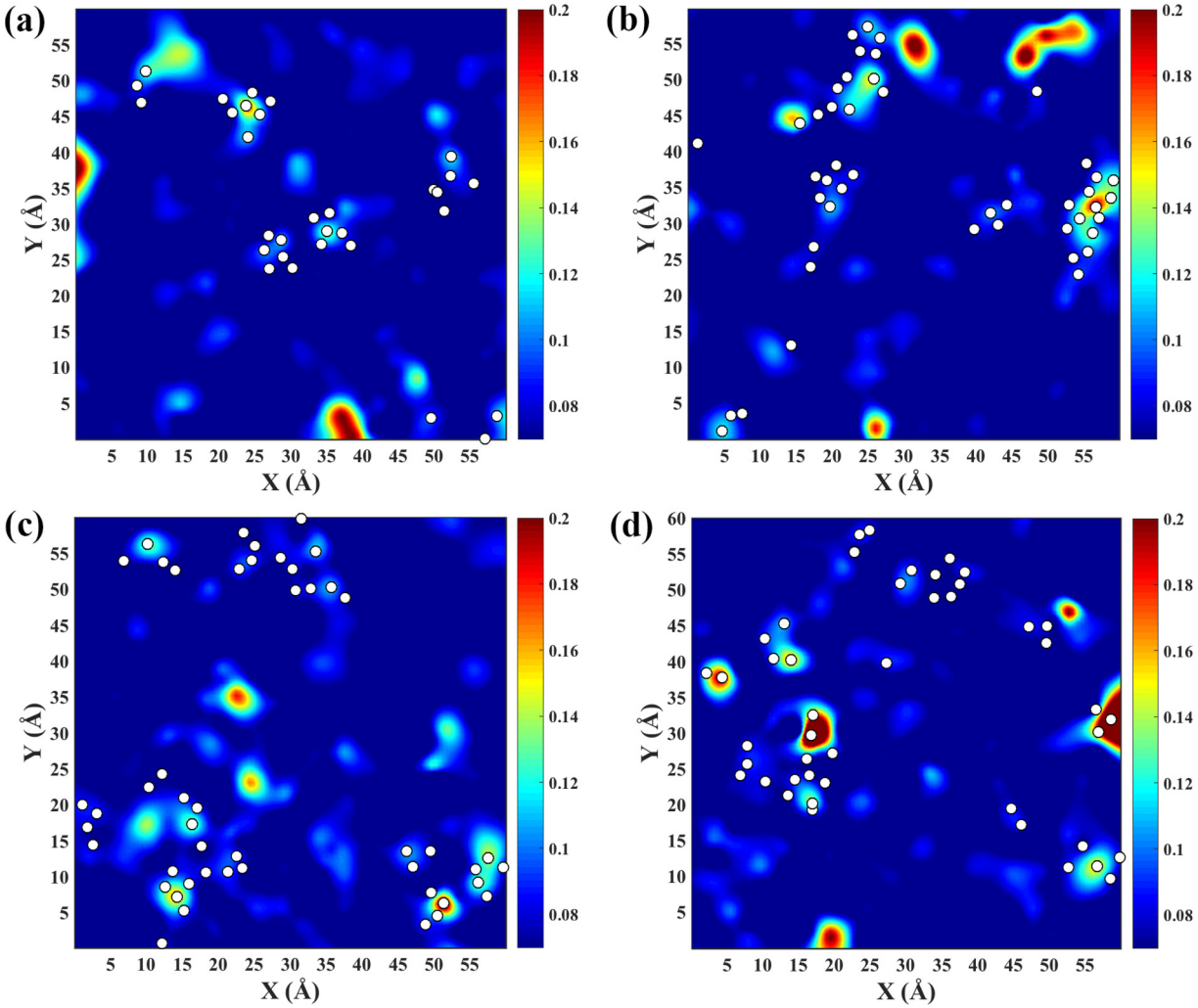

FIG. 6. Strong correlation between flexibility volume $v_{\text{flex},i}$ and the propensity for shear transformations. Contoured color maps show the spatial distribution of $v_{\text{flex},i}$ (see sidebar) in the a-Si quenched using a cooling rate of 5.0×10^{11}K/s. Four representative slabs [(a)–(d)] are sampled for illustration purposes and each has a thickness of 2.5 Å. White spots superimposed in the maps mark the locations of atoms that have experienced the most (top 5%) accumulative nonaffine displacement (D^2_{min}), upon athermal quasistatic shear of the simulation box to a global strain of 5%. Note that not all such regions would undergo shear transformation for a particular loading. This is reasonable because apart from the intrinsic flexibility of the local configurations, the stress field (tensor) is another (extrinsic) factor that will influence the response of the atoms.

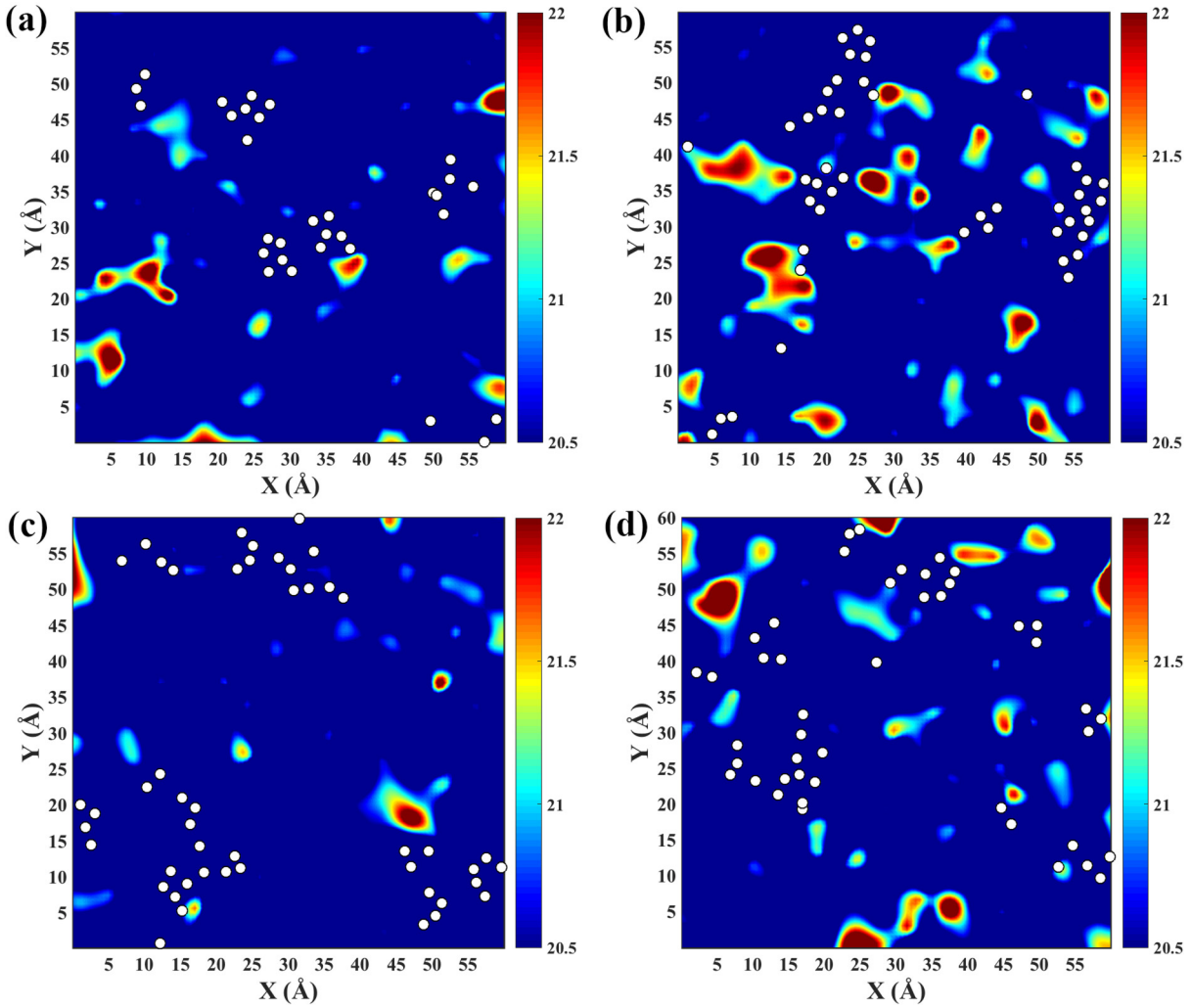

FIG. 7. Contour color maps showing the spatial distribution of local atomic volume ($\Omega_{a,i}$) (see colored sidebar for the magnitude) in the a-Si quenched using a cooling rate of 5.0×10^{11} K/s. Four representative slabs [(a)–(d)] are sampled for illustration purposes and each has a thickness of 2.5 Å. White spots superimposed in the maps mark the locations of atoms that have experienced the most (top 5%) accumulative nonaffine displacement (D^2_{min}), upon athermal quasistatic shear of the simulation box to a global strain of 5%. There appears to be no clear correlation with the locations with the highest local atomic volume.

D. Correlating υ_{flex} with local relaxation events

We first examine the correlation between flexibility volume and shear transformations, which are the fundamental processes underlying the inelastic deformation [41]. As already revealed in Refs. [7,37] and Fig. 2(b), a-Si samples with different quench rates show different propensity for shear deformation driven by imposed stresses (and flow stress and yield point); a slower cooling rate results in higher resistance to flow, in line with the higher G. Now the latter can be directly linked with a higher υ_{flex} (see Fig. 4). Moreover, we can use $\upsilon_{\text{flex},i}$ as an effective descriptor of local structure to offer a zeroth-order explanation of the different local response to the stress stimulus (longer-range collective effects on atomic motion in amorphous solids are neglected for the time being). Figures 6(a)–6(d) show that $\upsilon_{\text{flex},i}$ is indeed a very effective indicator of the propensity to undergo shear transformations. Specifically, here athermal quasistatic shearing (AQS) [42,43] was applied to induce atomic rearrangement in a-Si, and the shear transformations were tracked by monitoring the nonaffine displacement $D^2{}_{\text{min}}$ [43]. The contoured maps of the spatial distribution of $\upsilon_{\text{flex},i}$ are then compared/superimposed with the top 5% atoms that have experienced the most accumulative nonaffine strains, after a global strain (e.g., 5%). The clear correlation in Figs. 6(a)–6(d) establishes that under externally imposed stresses, shear transformations have a high propensity to originate from those regions with the highest flexibility volume [17]. Note that not all such regions would undergo shear transformation for a particular loading. This is reasonable because apart from the intrinsic flexibility of the local configurations, the stress field (tensor) is another (extrinsic) factor that will influence the response of the atoms. As presented in Fig. 7, such a correspondence with shear transformations is clearly absent, when a similar contour map is made to correlate with local atomic volume. This lack of correlation echoes our earlier statement that atomic volume is not a telltale structure parameter that connects well with the properties of a-Si.

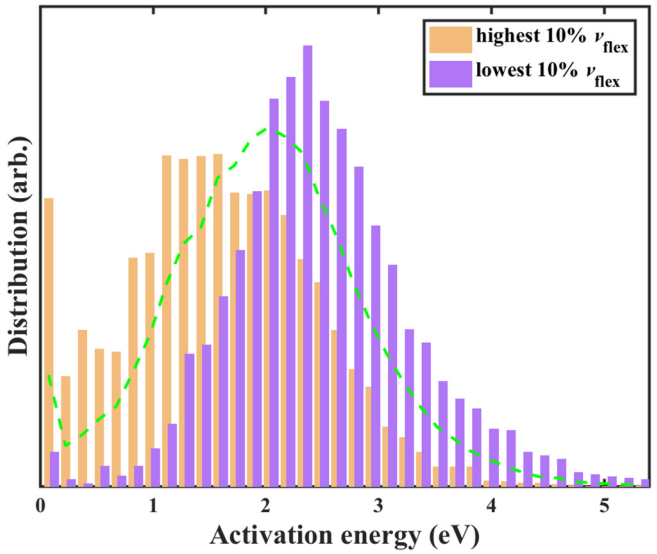

FIG. 8. Correlation between flexibility volume and thermally activated relaxation events. Distribution of activation energy in the a-Si (quenched with the cooling rate of 1.0×10^{11} K/s) characterized using ART nouveau. The activated relaxation events are for atoms in the center of their coordination polyhedra. This plot shows the distribution of activation energy for the two groups with the highest and lowest 10% flexibility volume ($\upsilon_{flex,i}$) and the green line is for the entire sample. Here each curve is normalized by the total number of activated events sampled by the entire group of atoms involved in the distribution.

In addition, it was found that the flexibility volume is also strongly correlated with the activation energy barrier for thermally activated relaxation events for a-Si, which can be monitored using the ART nouveau in MD simulations [17,26–28] (see Sec. II). The distribution of activation energy for all the atoms in the a-Si is shown as the dashed line in Fig. 8 (consistent with previous literature [44]). Then the atoms with the lowest 10% and highest 10% $\upsilon_{flex,i}$ are identified, and the distribution of activation energy for thermally activated events surrounding these atoms (as illustrated in Sec. II, small perturbations in ART were initially introduced on the designated atom and its nearest neighbors) is plotted. We observe in Fig. 8 that there is an obvious gap (a difference as large as ~1.1 eV) between the two peak positions for the two groups with the lowest 10% and highest 10% $\upsilon_{flex,i}$: the sites with larger flexibility volume are found to exhibit lower-energy barriers, and the lowest flexibility volume sites correspond to high-energy barriers. This clear bifurcation for thermally activated relaxation, based on $\upsilon_{flex,i}$ is also what was observed in the case of MGs [17].

E. General applicability of υ_{flex} for amorphous materials

Our results above have demonstrated the successful application of the new flexibility volume parameter for network-forming amorphous solids, using an a-Si model as the representative. Flexibility volume not only deterministically predicts the macroscopic shear modulus (Sec. III B), but also strongly correlates with the local relaxation events activated by shear stress or thermal agitation (Sec. III D). These findings, together with our previous work on MGs, point to the generality of the flexibility volume parameter for different amorphous materials, irrespective of their distinct structure and bonding characteristics. Therefore, flexibility volume as a descriptor of the structure state is projected to be universally useful for other amorphous materials, such as glassy polymers [45] and oxide glasses [46], to build a bridge between the structure and properties.

This general applicability is not possible with any previous indicator of the amorphous configuration. For example, one can again compare with previous parameters based on the magnitude of the local volume, such as the two-order-parameter (TOP) model proposed by Tanaka [47]. In this model, (i) there exist distinct locally favored structures (LFSs) as state F and (ii) such structures are formed in a "sea" of normal liquid structures (L). Each state is associated with a different value of energy (U), specific (or atomic) volume (V), and entropy (S). For amorphous or liquid Si [47], $U_F\langle U_L, V_F\rangle V_L$ (LFS with tetrahedral order has a higher specific volume) and $S_F < S_L$. For metallic glasses/liquids, however, $U_F < U_L$, $V_F < V_L$, $S_F < S_L$, because in this case the LFS is efficiently packed motifs with smaller volume. In both cases, the fraction of the LFS increases upon cooling, with lowered U and S. But V goes in the opposite direction between a-Si and MGs. Now, using flexibility volume rather than V, in both cases υ_{flex} consistently decreases with increasing undercooling and with decreasing cooling rate. As such, flexibility volume can act as a universal and quantitative descriptor of the LFS, or the structure state in general, in lieu of the static volume. In other words, specific LFSs can be vastly different for different glasses, such as tetrahedral order for a-Si versus icosahedral order for some MGs, but all LFSs inherently entail lower flexibility volume. This brings forth a unified description of atomic-level structure state for amorphous materials, despite their differences in chemical bonding and atomic packing.

IV. CONCLUDING REMARKS

We conclude by highlighting several salient features of our results. First of all, the correlation we have demonstrated above is an advance over relying solely on the static configuration (often merely a single aspect of the structure) to correlate with properties. Instead, our υ_{flex} purposely incorporates dynamics information via MSD and reflects the overall flexibility that is actually available in the glass internal structure. For a-Si, this descriptor implicitly covers information such as the nature of atomic bonding and how liquidlike the environment is. Although υ_{flex} does not directly describe anisotropy, it does reflect the effects of the latter on atomic flexibility. Second, the new flexibility parameter here arises from Debye theory and enables a quantitative calculation of G directly from Eq. (5). Currently none of the existing structural parameters for glasses incorporates dynamics and has one-to-one correspondence with key properties. Third, which is an important point of this work, the success with a-Si lends support to the universality of Eq. (5) for various types of glasses, beyond the demonstration earlier for metallic glasses [17]. In fact, the material we are modeling here is different in nearly all respects from the metallic glasses for which the formalism was initially developed: different from metallic glasses, a-Si is a network glass with directional covalent (rather than metallic)

bonding, and importantly, does not show the correlation of properties with free volume that we have grown to expect in metallic glasses. We have confirmed again that indeed excess volume is not of fundamental importance in governing the fertile sites where shear transformations tend to take place (see Fig. 7). Fourth, υ_{flex} is a good candidate as a single internal variable characterizing the state of the glass in a possible continuum description of mechanical rigidity. In the meantime, we also see that for this open-structure glass, high $\upsilon_{\text{flex},i}$ and its local average remain asa telltale indicator of regions most amenable to imposed local shape change via stress-driven shear transformations, as demonstrated by the correlation in Figs. 6(a)–6(d). $\upsilon_{\text{flex},i}$ is thus a prognostic parameter in monitoring the deformability distribution inside *a*-Si, to explain the spatial heterogeneity of the mechanical response in an amorphous solid [48–50]. Finally, our current approach of incorporating dynamics information overcomes some shortcomings associated with the earlier approach using the vibrational modes [43,51–53], where the soft spots were identified based on a preselected cut-off vibrational frequency (for example, arbitrarily choosing the 1% lowest frequency), and the participation of atoms in these soft modes is evaluated on a relative basis. This makes it difficult to decide which soft spots are truly eventful, in terms of being actually activated in relaxation. There is also no quantified measure of their contributions to the overall glass properties. Moreover, it is not feasible to directly compare the soft spots in different samples and in different glasses. In comparison, flexibility volume is universal and easier to use, and it quantitatively scales with G. One can now use this parameter to directly calculate and compare for different amorphous solids, and explain the spatial heterogeneity of mechanical properties mapped out for different local regions. Taken together, the new points made in this study constitute a step forward in developing (mathematically) verifiable correlations that link the amorphous configuration with properties.

ACKNOWLEDGMENTS

The work at JHU was supported by DoE-BES-DMSE under Grant No. DE-FG02-13ER46056. J.D. was supported at the Lawrence Berkeley National Laboratory by the U.S. Department of Energy, Office of Basic Energy Sciences, Materials Sciences and Engineering Division, through the Mechanical Behavior of Materials Program (KC13) under Contract No. DE-AC02-05CH11231. This work made use of resources of the National Energy Research Scientific Computing Center (NERSC), supported by the Office of Basic Energy Sciences of the U.S. Department of Energy under Contract No. DE-AC02-05CH11231.

[1] H. Matsumura and H. Tachibana, Amorphous silicon produced by a new thermal chemical vapor deposition method using intermediate species SiF_2, Appl. Phys. Lett. **47**, 833 (1985).
[2] H. Matsumura, Catalytic chemical vapor deposition (CTC–CVD) method producing high quality hydrogenated amorphous silicon, Jpn. J. Appl. Phys. **25**, L949 (1986).
[3] M. J. Kushner, A model for the discharge kinetics and plasma chemistry during plasma enhanced chemical vapor deposition of amorphous silicon, J. Appl. Phys. **63**, 2532 (1988).
[4] H. A. Atwater and W. L. Brown, Grain boundary mediated amorphization in silicon during ion irradiation, Appl. Phys. Lett. **56**, 30 (1990).
[5] S. Roorda, W. Sinke, J. Poate, D. Jacobson, S. Dierker, B. Dennis, D. Eaglesham, F. Spaepen, and P. Fuoss, Structural relaxation and defect annihilation in pure amorphous silicon, Phys. Rev. B **44**, 3702 (1991).
[6] Y.-C. Wang, W. Zhang, L.-Y. Wang, Z. Zhuang, E. Ma, J. Li, and Z.-W. Shan, *In situ* TEM study of deformation-induced crystalline-to-amorphous transition in silicon, NPG Asia Mater. **8**, e291 (2016).
[7] M. J. Demkowicz and A. S. Argon, High-Density Liquidlike Component Facilitates Plastic Flow in a Model Amorphous Silicon System, Phys. Rev. Lett. **93**, 025505 (2004).
[8] M. J. Demkowicz and A. S. Argon, Autocatalytic avalanches of unit inelastic shearing events are the mechanism of plastic deformation in amorphous silicon, Phys. Rev. B **72**, 245206 (2005).
[9] M. H. Cohen and G. Grest, Liquid-glass transition, a free-volume approach, Phys. Rev. B **20**, 1077 (1979).
[10] A. R. Yavari, A. Le Moulec, A. Inoue, N. Nishiyama, N. Lupu, E. Matsubara, W. J. Botta, G. Vaughan, M. Di Michiel, and Å. Kvick, Excess free volume in metallic glasses measured by X-ray diffraction, Acta Mater. **53**, 1611 (2005).
[11] T. K. Haxton and A. J. Liu, Activated Dynamics and Effective Temperature in a Steady State Sheared Glass, Phys. Rev. Lett. **99**, 195701 (2007).
[12] G. Kumar, P. Neibecker, Y. H. Liu, and J. Schroers, Critical fictive temperature for plasticity in metallic glasses, Nat. Commun. **4**, 1536 (2013).
[13] Y. Guo, A. Morozov, D. Schneider, J. W. Chung, C. Zhang, M. Waldmann, N. Yao, G. Fytas, C. B. Arnold, and R. D. Priestley, Ultrastable nanostructured polymer glasses, Nat. Mater. **11**, 337 (2012).
[14] H. B. Yu, Y. Luo, and K. Samwer, Ultrastable metallic glass, Adv. Mater. **25**, 5904 (2013).
[15] R. Xue, L. Zhao, C. Shi, T. Ma, X. Xi, M. Gao, P. Zhu, P. Wen, X. Yu, and C. Jin, Enhanced kinetic stability of a bulk metallic glass by high pressure, Appl. Phys. Lett. **109**, 221904 (2016).
[16] F. H. Stillinger and T. A. Weber, Computer simulation of local order in condensed phases of silicon, Phys. Rev. B **31**, 5262 (1985).
[17] J. Ding, Y.-Q. Cheng, H. Sheng, M. Asta, R. O. Ritchie, and E. Ma, Universal structural parameter to quantitatively predict metallic glass properties, Nat. Commun. **7**, 13733 (2016).
[18] W. H. Zachariasen, The atomic arrangement in glass, J. Am. Chem. Soc. **54**, 3841 (1932).
[19] M. Treacy and K. Borisenko, The local structure of amorphous silicon, Science **335**, 950 (2012).
[20] N. Mousseau and L. J. Lewis, Topology of Amorphous Tetrahedral Semiconductors on Intermediate Length Scales, Phys. Rev. Lett. **78**, 1484 (1997).

[21] Y. Cheng and E. Ma, Atomic-level structure and structure–property relationship in metallic glasses, Prog. Mater. Sci. **56**, 379 (2011).
[22] M. P. Allen and D. J. Tildesley, *Computer Simulation of Liquids* (Oxford University Press, New York, 1989).
[23] C. Fusco, T. Albaret, and A. Tanguy, Role of local order in the small-scale plasticity of model amorphous materials, Phys. Rev. E **82**, 066116 (2011).
[24] A. Widmer-Cooper and P. Harrowell, Predicting the Long-Time Dynamic Heterogeneity in a Supercooled Liquid on the Basis of Short-Time Heterogeneities, Phys. Rev. Lett. **96**, 185701 (2006).
[25] K. Tsumuraya, K. Ishibashi, and K. Kusunoki, Statistics of Voronoi polyhedra in a model silicon glass, Phys. Rev. B **47**, 8552 (1993).
[26] R. Malek and N. Mousseau, Dynamics of Lennard-Jones clusters: A characterization of the activation-relaxation technique, Phys. Rev. E **62**, 7723 (2000).
[27] D. Rodney and C. Schuh, Distribution of Thermally Activated Plastic Events in a Flowing Glass, Phys. Rev. Lett. **102**, 235503 (2009).
[28] Y. Fan, T. Iwashita, and T. Egami, How thermally activated deformation starts in metallic glass, Nat. Commun. **5**, 5083 (2014).
[29] M. Zink, K. Samwer, W. Johnson, and S. Mayr, Plastic deformation of metallic glasses: Size of shear transformation zones from molecular dynamics simulations, Phys. Rev. B **73**, 172203 (2006).
[30] M. J. Demkowicz, Mechanisms of plastic deformation in amorphous silicon by atomistic simulation using the Stillinger-Weber potential, Ph.D. thesis, Massachusetts Institute of Technology, 2005.
[31] T. Albaret, A. Tanguy, F. Boioli, and D. Rodney, Mapping between atomistic simulations and Eshelby inclusions in the shear deformation of an amorphous silicon model, Phys. Rev. E **93**, 053002 (2016).
[32] W. H. Wang, The elastic properties, elastic models and elastic perspectives of metallic glasses, Prog. Mater. Sci. **57**, 487 (2012).
[33] W. L. Johnson, M. D. Demetriou, J. S. Harmon, M. L. Lind, and K. Samwer, Rheology and ultrasonic properties of metallic glass-forming liquids: A potential energy landscape perspective, MRS Bull. **32**, 644 (2007).
[34] J. Ding, Y.-Q. Cheng, and E. Ma, Full icosahedra dominate local order in $Cu_{64}Zr_{34}$ metallic glass and supercooled liquid, Acta Mater. **69**, 343 (2014).
[35] U. Buchenau, R. Zorn, and M. A. Ramos, Probing cooperative liquid dynamics with the mean square displacement, Phys. Rev. E **90**, 042312 (2014).
[36] J. A. Reissland, *The Physics of Phonons* (Wiley-Interscience, New York, 1973).
[37] M. J. Demkowicz and A. S. Argon, Liquidlike atomic environments act as plasticity carriers in amorphous silicon, Phys. Rev. B **72**, 245205 (2005).
[38] P. J. Caplan, E. H. Poindexter, B. E. Deal, and R. R. Razouk, ESR centers, interface states, and oxide fixed charge in thermally oxidized silicon wafers, J. Appl. Phys. **50**, 5847 (1979).
[39] G. Van den Hoven, Z. Liang, L. Niesen, and J. Custer, Evidence for Vacancies in Amorphous Silicon, Phys. Rev. Lett. **68**, 3714 (1992).
[40] S. T. Pantelides, Defects in Amorphous Silicon: A New Perspective, Phys. Rev. Lett. **57**, 2979 (1986).
[41] M. Tsamados, A. Tanguy, C. Goldenberg, and J.-L. Barrat, Local elasticity map and plasticity in a model Lennard-Jones glass, Phys. Rev. E **80**, 026112 (2009).
[42] C. E. Maloney and A. Lemaître, Amorphous systems in athermal, quasistatic shear, Phys. Rev. E **74**, 016118 (2006).
[43] J. Ding, S. Patinet, M. L. Falk, Y. Cheng, and E. Ma, Soft spots and their structural signature in a metallic glass, Proc. Natl. Acad. Sci. USA **111**, 14052 (2014).
[44] H. Kallel, N. Mousseau, and F. Schiettekatte, Evolution of the Potential-Eneergy Surface of Amorphous Silicon. Phys. Rev. Lett. **105**, 045503 (2010).
[45] D. N. Theodorou and U. W. Suter, Detailed molecular structure of a vinyl polymer glass, Macromolecules **18**, 1467 (1985).
[46] B. E. Warren and J. Biscce, The structure of silica glass by x-ray diffraction studies, J. Am. Ceram. Soc. **21**, 49 (1938).
[47] H. Tanaka, Bond orientational order in liquids: Towards a unified description of water-like anomalies, liquid-liquid transition, glass transition, and crystallization, Eur. Phys. J. E **35**, 1 (2012).
[48] A. Argon, Plastic deformation in metallic glasses, Acta Metall. **27**, 47 (1979).
[49] E. Ma and J. Ding, Tailoring structural inhomogeneities in metallic glasses to enable tensile ductility at room temperature, Mater. Today **19**, 568 (2016).
[50] E. Bouchbinder, J. S. Langer, and I. Procaccia, Athermal shear-transformation-zone theory of amorphous plastic deformation. I. Basic principles, Phys. Rev. E **75**, 036107 (2007).
[51] M. L. Manning and A. J. Liu, Vibrational Modes Identify Soft Spots in a Sheared Disordered Packing, Phys. Rev. Lett. **107**, 108302 (2007).
[52] A. Tanguy, B. Mantisi, and M. Tsamados. Vibrational modes as a predictor for plasticity in a model glass, Europhys. Lett. **90**, 16004 (2010).
[53] K. Chen, M. L. Manning, P. J. Yunker, W. G. Ellenbroek, Z. Zhang, A. J. Liu, and A. G. Yodh, Measurement of Correlation Between Low-Frequency Vibrational Modes and Particle Rearrangements in Quasi-Two-Dimensional Colloidal Glasses, Phys. Rev. Lett. **107**, 108301 (2011).